DRYING OF SOLUTIONS AND SUSPENSIONS IN THE MODIFIED SPOUTED BED WITH DRAFT TUBE

by

Zorana Lj. ARSENIJEVIĆ, Željko B. GRBAVČIĆ, and Radmila V. GARIĆ-GRULOVIĆ

Original scientific paper
UDC: 532.546:66.047.7/.8
BIBLID: 0354–9836, *6* (2002), 2, 47-70

A modified spouted bed dryer with inert particles was used for drying of solutions and suspensions. The effects of the operating conditions on dryer throughput and product quality were investigated. Experiments were performed in a cylindrical column 215 mm in diameter and 1150 mm in height with a draft tube 70 mm in diameter and 900 mm length. The bed was made of polyethylene particles 3.3 mm in diameter and of density of 921 kg/m^3. The pesticide Cineb, inorganic compound calcium carbonate, organic compound calcium stearate, and pure water were used as feeding materials.

A drying model using the continuity and momentum equations for turbulent accelerating two-phase flow and conventional rate equations is proposed and discussed. The work is relevant for estimating dryer performance.

Key words: spouted bed, drying, solid-water solutions, suspensions

Introduction

Drying of solutions and suspensions is the very important process in the chemical, pharmaceutical and food processing industries. This unit operation is most energy consuming industrial operation. Although there are hundreds of variants actually used in drying, the research efforts over the world are associated with the development of more sophisticated systems. In general, the trends in drying technology are associated with higher energy efficiency, enhanced drying rates and development of more compact dryers, better control for enhanced quality and optimal capacity, developments of multi-processing units (for example filter-dryer), *etc*. Mujumdar [1] pointed out that numerous new or improved drying technologies are currently at various stages of development. Over 400 dryer types have been cited in the technical literature although only about 50 types are commonly found in practice. The selection criterion is a complex process, which is not entirely scientific but also involves subjective judgment as well as considerable empiricism. It should also be noted that the pre-drying as well as

post-drying stages have important bearing on the selection of appropriate dryer types for a given application. Each type of dryer has specific characteristics, which make it suited or unsuitable for specific applications [2].

Generally, an efficient drying system should meet several conditions: high values of heat and mass transfer coefficients, high contact area, high input of heat carrier gas, uniform temperature distribution over the drying chamber, the use of concentrated suspensions (as high as possible) in order to minimize water amount which should be evaporated and the use high inlet air temperature, as much as possible. However, many of these conditions are conflict each to other. The only drying concept that meets majority of the mentioned conditions is drying in an agitated bed of inert particles.

Drying of slurries on inert particles is a relatively novel technology to produce powdery materials. It was originally developed for drying of pigments, chemicals and some biomaterials to eliminate constrains of spray, drum and paddle dryers. Classical fluid bed, spouted bed, spout-fluid bed, jet spouted bed and vibrated fluid bed are the most popular dryers used for drying on inert particles [3-5]. Independently of the hydrodynamic configuration of the dryer, the principle behind this technology is based on the drying of a thin layer of the slurry that coats the surface of inert particles. Depending on the dryer type, these particles can be vibrated, fluidized or spouted either by hot air only, or in combination with a mechanical device installed within the dryer, such as an agitator or conveyor screw. Several systems (fluidized, spouted, spout-fluid and their different modifications) are at various stages of development [1, 6-11].

The extensive introduction of the fluidization into drying processes resulted from the several principal advantages. With respect to the main efficiency criteria, *i. e.* specific water evaporation rate, specific heat consumption and specific air consumption, a fluidized bed dryer with inert particles represents a very attractive alternative to other drying technologies. A high drying efficiency results from the large contact area and from the large temperature difference between the inlet and outlet air. A rapid mixing of the particles, due to aggregative fluidization leads to nearly isothermal conditions throughout the bed.

In our prior investigations, a fluid bed dryer with inert particles was used for drying of solutions, suspensions and pastes, as described in detail in our recent work [12]. The drying chamber is the cylindrical column of stainless steel D_c = 215 mm i. d. in the lower part and 350 mm i. d. in the upper part. The overall column height was 1210 mm, where the effective column height (above distributor) was 900 mm. The inert particles were glass spheres with the mean diameter d_p = 1.9 mm (density 2460 kg/m^3) and d_p = = 0.925 mm (density 2640 kg/m^3). The inert bed mass of larger glass particles was 6.79 kg, static bed height was 122 mm and the total inert particle area was 8.54 m^2, while for the smaller particles these values were 4.52 kg, 80 mm and 11.12 m^2, respectively. Minimum fluidization velocity was determined at ambient air temperature using standard procedure (U_{mF} = 0.955 m/s for particles of d_p = 1.9 mm, and U_{mF} = 0.61 m/s for particles of d_p = 0.925 mm). Superficial fluid velocity U (at ambient temperature) was varied between 1.48 and 2.30 m/s (*i. e*. fluidization number was 1.55-3.77), inlet air

temperature T_{gci} between 175 and 366 °C, drying temperature T_{gce} was in range of 65.9 and 122 °C, and water contents x_{H_2O}, in the feed materials varies between 0.40 and 0.75 kg_{H_2O}/ kg_{sus} .

The feed material is directly supplied into the column using the peristaltic pump for suspensions and the screw transporter for pastes. The automatic control system of bed temperature is directly connected with the feeding system. The product is separated from the exhaust air by the cyclone and bag filters.

The drying mechanism is consisted from three steps, which simultaneously occur in the different region of the bed. The drying mechanism depends of the feed slurry density and consistency. If the feed is relatively dilute slurry, the drying mechanism consists of three steps, which occur simultaneously in the different regions of the bed. The supplied solution or suspension form film and adhere to the surface of inert particles. Because of very large surface area of inert particles and intensive fluidization, the moisture is removed in very short time. Solids remaining on the surface of inert particles are peeled off by the friction and collision. Finally, the product powder is elutriated from the inert bed by the exhaust air. If the feed is a paste (dense slurry) then wet paste aggregates fluidize together with the inert particles. During the drying process, the size of the aggregates decreases due to the elutriation of dried particles from the surface. Due to the rapid mixing of inert particles the bed temperature is approximately uniform.

Drying tests were performed continuously. In our fluidized bed dryer were successfully treated suspensions and very dense pastes, the fungicides and pesticides (Cineb, Ciram, Propineb, Mangoceb, copper hydroxide, copper oxy-chloride, copper oxy-sulphate), other inorganic compounds (calcium carbonate, calcium sulphate, cobalt carbonate, electrolytic copper, sodium chloride), complex compound (organo--bentonite). Suspension and product hold-up in the bed varies between 6 and 8% by mass and the product with the same particle size as raw material is obtained. During drying of above-mentioned materials, it was observed that the bed temperature rapidly decreases above bed distributor approaching nearly constant temperature over the major bed portion. In addition, it was noticed that decreasing the bed temperature bellow about 60 °C increases residual water content in the dried product. In these drying tests, the residual water content in the powdery products mainly was at desired level (beneath 1%). The simple one-dimensional mathematical model, based on overall heat balance, fairly well simulates dryer operation.

Drying in fluidized bed of inert particles is simple and very efficient technique. The most important disadvantage of this system lies in possibility of bed sintering in certain applications. For example, the experimental trials of drying several organic and biological materials such as calcium stearate, tartaric acid, brewery yeast, soya milk and their mixtures, liposome, tomato pulp, raw eggs, starch, were unsuccessful. Application of fluidized bed in drying of such materials that contain carbohydrates or fats is not

possible because it's adhesiveness leads to unstable operation, *i. e*. with time the inert particles motion becomes slower and slower afterwards the bed usually is blocked.

The most commonly used equipment for drying such materials is a spray dryer. An alternative to a spray dryer is the spouted and modificated spouted bed dryer, which combined features of both spray dryers and fluidized bed dryers.

Drying in the spouted bed dryer with draft tube

A schematic diagram of the spouted bed with a draft tube (DTSB) is given in Fig. 1. The spouted bed with a draft tube is a modification of classical spouted bed developed in order to improve operability and to provide better agreement between bed characteristics and process requirements.

Spouting has been studied as operation for contacting fluid and coarse particles (d_p > 1 mm) 13 . A spouted bed can be formed in vertical column where the fluid jet blows vertically upwards along the centerline of the column thus forming a spout in which there are fast moving fluid and entrained particles. The remainder of the particles bed, the annulus between spout and the column wall, is densely packed with particles moving slowly downwards and radially inwards. Air percolates through these particles from the spout. The main disadvantage of spouted bed system is high pressure drop due to the expansion and friction through the inlet nozzle. For example, in 0.91 m in diameter spouted bed the pressure drop through the inlet section only can be up to few times higher than pressure drop through the bed only. This high pressure drop is due to the fact that all of the air is forced into the bed through inlet nozzle, although this air after short part of the bed flows mainly through the annular region.

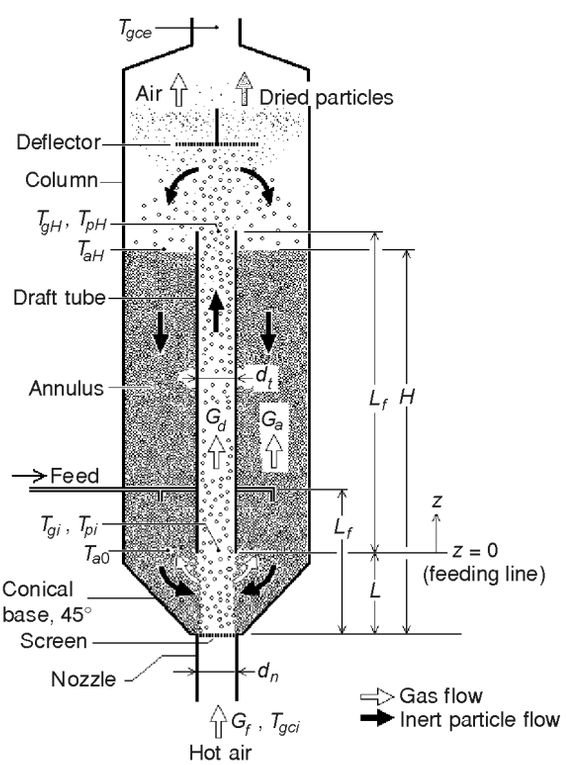

Figure 1. Schematic diagram of the modified spouted bed with draft tube (DTSB)

The use of a draft tube in the central region of the spouted

bed causes a modification of the normal flow patterns in the bed. Namely, the bed is divided in two zones: a pneumatic transport of particles in the draft tube and nearly plug flow of moving bed in the annular region, since the draft tube forces all of the particles to travel through the entire annulus section before reentering the spout. The overall pressure drop in large systems is much less than in conventional spouted bed.

Particle circulation rate and minimum fluid velocity for the circulation are smaller than in a conventional spouted bed. Although these modifications of the bed structure are not generally desirable for all of possible processes in spouted and spout-fluid beds, there are several processes for which this system can be applied (drying of particles, drying of solutions, granulation, thermal disinfestations, blending, *etc.*) since system characteristics can be in accordance with the process characteristics. In DTSB there is no height limitation (*H*, Fig. 1) imposed by the maximum spoutable bed height that exist in a conventional spouted bed. Another modification of DTSB is so called modified draft tube spout-fluid bed (DTSFB). In this system, a part of the fluid is directly introduced into annular section through the perforated cone. Detailed informations about DTSB and DTSFB can be found elsewhere 14, 15 .

When DTSB or DTSFB is used as suspension and slurry dryer, the feed can be sprayed at the top of the annulus or directly at the entrance region just bellow the draft tube inlet. Another way is to pump suspension or slurry directly into the annulus section at several points. Essentially inert particle is coated by the thin film of suspension or slurry. Wet particles enter the draft tube and dry as they fly upward at high velocity entrained by the gas. The drying process continues, until the moisture content drops to a critical value at which the coat is dry enough to become brittle. This dry coat is then broken and peeled off from the solid surface due to particle-particle collisions, and particle collisions with the deflector. The inert particles must be surface dry when they fall back on to the annulus section to prevent their sticking together and bed sintering. Stable operation of the draft tube spouted bed is attained when the rate of dry layer removal is equal or greater than the material feeding rate.

The spout-fluid bed with draft tube has been used by Povrenović and associates 16-18 for drying various solutions and suspensions. Experimental unit was a column of 0.25 m diameter, an inlet nozzle of 0.05 m diameter, a cone angle 45° and draft tube of 0.06 m diameter and 0.6 m length, which was mounted axially above the nozzle with a possibility to change the distance from the bottom of the column. The polypropylene beads of 3.6 mm mean diameter and density 900 kg/m^3 or the polyethilentheraphtalat particles of 2.5 mm mean diameter and density 1390 kg/m^3 were used as inert particles. Hot air was introduced through a nozzle at the bottom of the column. Additional hot air was introduced into the bed through a perforated conical bottom. The suspension to be dried was sprayed onto the top of the annulus or from the bottom of the column by twin fluid nozzles. The wide range of materials which were dried in above described dryer include animal blood plasma, brewery yeast, skim milk, starch, red beet juice, carrot juice, soya milk and some of theirs combinations.

In this work, a modified spouted bed dryer with inert particles was used for drying of solutions and suspensions. The effects of the operating conditions on dryer throughput and product quality were investigated. A model for predicting dryer behavior is presented and discussed.

Mathematical model of drying in the DTSB

Hydrodynamic modeling

The one-dimensional model of accelerating turbulent gas-solid dilute phase flow of coarse particles was formulated and experimentally verified in pervious investigations 19-21 . The theoretical bases of the model were the continuity and momentum equations for the fluid and particle phases variational model for calculating the fluid-particle interphase drag coefficient. The model predicts particle velocity, voidage, solids flowrate and the pressure gradient quite well. The draft tube in our dryer is essentially a pneumatic riser, which is relatively short, so accelerating two-phase flow equations must be used to model hydrodynamics.

The one-dimensional mixture momentum equation is (Leung 22):

$$\rho_f \frac{d}{dz}(\varepsilon u^2) \quad \rho_p \frac{d}{dz}[(1 \quad \varepsilon)v^2] \qquad \frac{d}{dz} \quad [(\rho_f (1 \quad \varepsilon) \quad \rho_f \varepsilon]g \quad F_f \quad F_p \tag{1}$$

The individual momentum balances for the fluid and particle phases (Nakamura and Capes 23) are:

$$\rho_f \frac{d}{dz}(\varepsilon u^2) \quad \varepsilon \quad -\frac{dp}{dz} \quad \varepsilon\rho_f g \quad \beta(u \quad v)^2 \quad F_f \tag{2}$$

$$\rho_p \frac{d}{dz}[(1 \quad \varepsilon)v^2] \quad (1 \quad \varepsilon) \quad \frac{dp}{dz} \quad \beta(u \quad v)^2 \quad \rho_p g(1 \quad \varepsilon) \quad F_p \tag{3}$$

where $\beta(u - v)^2$ $(= F_D)$ is the hydrodynamic drag force per unit volume of suspension. F_f and F_p are pressure losses due to fluid-wall and particle-wall friction written in terms of friction factors f_f and f_p:

$$F_f \quad 2f_f \rho_f U^2 / d_t \tag{4}$$

$$F_p \quad 2f_p \rho_p (1 \quad \varepsilon)v^2 / d_t \tag{5}$$

The continuity equations for the gas and particle phases are:

$$\frac{d}{dz}(u\varepsilon) \quad 0 \quad i.e. \quad u\varepsilon \quad \frac{G_d}{\rho_f A_t} \quad U \tag{6}$$

$$\frac{d}{dz}[v(1 \quad \varepsilon)] \quad 0 \quad i.e. \quad v(1 \quad \varepsilon) \quad \frac{G_p}{\rho_p A_t} \quad c_s \tag{7}$$

Fluid-particle interphase drag coefficient, fluid-wall and particle-wall friction coefficient

The dimensionless fluid-particle interphase drag coefficient determined from the authors' variational model [21] is:

$$\frac{\beta}{\beta_{mF}} \quad 1 \quad C_2 \quad \frac{1}{\lambda} \; 1 \quad \lambda \frac{\varepsilon \quad \varepsilon_{mF}}{1 \quad \varepsilon_{mF}} \quad C_1 \Big)^{2} \Big)^{1/2} \tag{8}$$

where the constants C_1, C_2, and λ are:

$$C_1 \quad [1 \quad (U_{mF}^2 / \varepsilon_{mF}^3 U_t^2)^2]^{1/2} \tag{9}$$

$$C_2 \quad \frac{1}{\lambda}\sqrt{1 \quad C_1^2} \tag{10}$$

$$\lambda \quad \sqrt{1 \quad C_1^2} \quad C_1 \tag{11}$$

and

$$\beta_{mF} \quad \frac{\varepsilon_{mF}^3 (1 \quad \varepsilon_{mF}) g(\rho_p \quad \rho_f)}{U_{mF}^2} \tag{12}$$

Fluid-wall friction term (F_f) was determined using eq. (4) and a standard friction factor correlation [24]:

$$F_f = 0.0791/\mathrm{Re}^{0.25} \tag{13}$$

where Reynolds number is based on superficial gas velocity ($\mathrm{Re} = d_t \rho_f U/\mu$).

A particle-wall friction term was correlated in our non-accelerating experiments [20]:

$$f_p \frac{\varepsilon^3}{1 \quad \varepsilon}\frac{U}{U_t} \quad 0.0017 \quad \frac{1 \quad \varepsilon}{u_s / U_t}^{1.5} \tag{14}$$

For a known fluid superficial velocity and particle mass flowrate, continuity equations and momentum balances could be integrated numerically in order to obtain the axial variation of particle velocity, voidage and pressure gradient in the transport tube ($z > 0$, Fig. 1).

Using the continuity above the feeding point (z > 0) momentum balances (eqs. 1 and 2) become:

$$\frac{dp}{dz} = \frac{1}{\varepsilon}\beta(u - v)^2 - \rho_f g\varepsilon - F_f - \rho_f u^2 \frac{d\varepsilon}{dz} \tag{15}$$

$$\frac{dp}{dz} = [\rho_p(1 - \varepsilon) - \rho_f\varepsilon]g - F_f - F_p - \gamma\frac{d\varepsilon}{dz} \tag{16}$$

where

$$\gamma = \rho_p v^2 - \rho_f u^2 \tag{17}$$

From eqs. (15) and (16) we get:

$$\frac{d\varepsilon}{dz} = \frac{\beta(u - v)^2 - \varepsilon[(\rho_p - \rho_f)g(1 - \varepsilon) - F_f] - F_f(1 - \varepsilon)}{\gamma\varepsilon - \rho_f u^2} \tag{18}$$

Numerical solution of eq. (18) gives the voidage distribution along the tube. In this calculation F_f is obtained using eqs. (4) and (13), F_p is obtained using eqs. (5) and (14) while β is obtained from eq. (8). The gas and particle phase velocities are then calculated from continuity (eqs. 6 and 7) and $-dp/dz$ is calculated using eq. (15) or (16). The boundary condition for eq. (18) is the voidage at the feeding line ε_0. Numerical integration of the calculated pressure gradient along the transport line axis gives the axial pressure distribution. In these calculations, the boundary condition was the fluid pressure at the top of the transport tube (p_H).

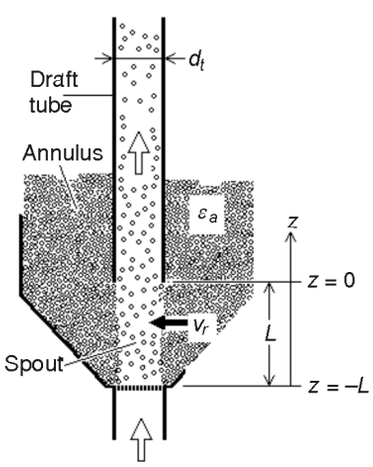

Figure 2. Schematic diagram of the inlet section to the draft tube

Boundary conditions

Transport line inlet conditions in general are dependent on the configuration of the feeder to the transport line. The present analysis is restricted to the use of spouted or spout-fluid beds as a feeding device to the draft tube. Figure 2 gives the schematic diagram of the inlet region. The section between $z = -L$ and $z = 0$ is almost identical to the inlet region of a spouted or spout-fluid bed. The fluid jet penetrates upward along the central line, forming a spout and entraining the particles up the spout. The annulus between the spout and the hopper wall is a densely packed bed with particles moving slowly downwards and radially inward toward the spout.

Observations of the inlet section of the spouted bed using high speed photography Thorley *et al.* [25] and Lefroy and Davidson [26] show that spout walls were continually collapsing near the base and particles were being swept into the fluid jet. With

increase in axial distance, the effect of collisions is significant, but this effect is minor when a spouted bed is used as feeder due to the short spout (low draft tube spacing, L). For this reason, radial particle velocity at the spout-annulus interface (v_r, Fig. 2) is assumed to be constant between $z = -L$ and $z = 0$. Assuming that "spout" diameter is approx- imately constant and equal to the draft tube diameter, we have:

$$G_p \quad \rho_p A_t c_s \quad \int_L^0 \rho_p v_r (1 \quad \varepsilon_a) \pi d_t dz \quad \rho_p v_r (1 \quad \varepsilon_a) \pi d_t L \tag{19}$$

where ε_a is the voidage of the moving packed bed surrounding the spout, which is also constant. By continuity between $z = -L$ and $z = 0$ we have:

$$A_t \frac{d}{dz}[v(1 \quad \varepsilon)] \quad v_r (1 \quad \varepsilon_a) \pi d_t \tag{20}$$

From eqs. (19 and 20) it follows that the solids superficial velocity varies linearly with height in the inlet section to the transport tube, *i. e.* between $z = -L$ and $z = 0$:

$$v(1 \quad \varepsilon) \quad c_s \frac{z}{L} \tag{21}$$

By differentiation of eq. (21):

$$(1 \quad \varepsilon)\frac{dv}{dz} \quad v\frac{d\varepsilon}{dz} \quad \frac{c_s}{L} \tag{22}$$

In the spout, the radially averaged particle velocity increases from 0 at $z = -L$ up to the final transport velocity at the end of the acceleration zone, which is well above feeding line. However, the radially averaged particle concentration $(1 - \varepsilon)$ increases from 0 at $z = -L$ up to ε_0 at $z = 0$ and then starts to decrease. At the end of the acceleration zone solids concentration becomes equal to the final transport concentration. It is reasonable to assume that:

$$\left.\frac{d\varepsilon}{dz}\right|_{z \quad 0} \quad 0 \tag{23}$$

Mathematically we treated the feeding line as a left boundary ($z = 0^-$). From eqs. (22) and (23) it follows that:

$$\left.\frac{dv}{dz}\right|_{z \quad 0} \quad \frac{c_s}{L(1 \quad \varepsilon_0)} \tag{24}$$

By substituting eqs. (23) and (24) into eqs. (2) and (3) applied to the feeding line, we get:

$$\left.\frac{dp}{dz}\right|_{z \quad 0} \quad \frac{\beta(u_0 \quad v_0)^2 \quad \rho_f g \varepsilon_0 \quad F_f}{\varepsilon_0} \tag{25}$$

$$\left.\frac{dp}{dz}\right|_{z \quad 0} \quad [\rho_p(1 \quad \varepsilon_0) \quad \rho_f \varepsilon_0]g \quad F_p \quad F_f \quad 2\frac{\rho_p c_s^2}{L(1 \quad \varepsilon_0)} \tag{26}$$

For a known fluid superficial velocity (U) and solids superficial velocity (c_s) eqs. (25) and (26) gives solutions for $(-dp/dz)_0$ and ε_0 at $z = 0^-$. In this calculation F_f is obtained using eqs. (4) and (13), F_p is obtained using eqs. (5) and (14) while β is obtained from eq. (8). The gas and particle phase velocities are then calculated from continuity (eqs. 6 and 7):

$$G_f = G_d + G_a \tag{27}$$

Since in DTSB air introduced into column partially penetrate into the annulus, air mass flowrate through the draft tube was determined using material balance.

Mass flowrate of the air through the annulus section (G_a) was determined indirectly by measuring pressure gradient in the annulus in each run and using an experimentally determined correlation pressure gradient *vs.* Reynolds number.

Mass and heat transfer modeling

The assumptions of the mass and heat transfer model are:

- drying of solutions or suspensions started at the feeding point at the bottom of the draft tube (z = 0),
- liquid phase forms uniform film around the inert particle, and
- liquid film, inert particle and dry mater are at the same temperature.

The mass flux of moisture (water) evaporating at the surface of the inert polyethylene particles is related to its mass transfer coefficient by the equation:

$$G_{sv}(1 \quad y)dy \quad \frac{h_D M_R}{RT_g} a_p A_t (p_s \quad p_B)dz \tag{28}$$

where p_S is function of the fluid temperature.

The surface air humidity (at the T_p) and partial water pressure in the bulk are given by:

$$y \quad \frac{0.662\varphi p_s(T_p)}{p \quad \varphi p_s(T_p)} \tag{29}$$

$$p_s \quad \frac{yp}{0.662 \quad y} \tag{30}$$

Specific surface area of bed of inert particles is:

$$a_p \quad \frac{6(1 \quad \varepsilon)\psi}{d_p} \tag{31}$$

The gas phase temperature change is the result of heat transferred to the liquid film covering the inert particles:

$$G_{sv}(1 \quad y)c_{pg} \frac{dT_g}{dz} \quad h_p a_p A_t (T_g \quad T_p) \tag{32}$$

The gas phase gives heat for heating inert particles, water film, dry mater from suspension and water phase evaporation:

$$G_{sv}(1 \quad y)c_{pg}\frac{dT_g}{dz} \quad [G_p c_{ps} \quad G^L_{\mathrm{H_2O}} c_{pL} \quad G_{sm} c_{pm}]\frac{dT_p}{dz} \quad G_{sv} r_{\mathrm{H_2O}} \frac{dy}{dz} \tag{33}$$

The gas-particle heat transfer correlation used was [27]

$$\mathrm{Nu}_p \quad 2 \quad 0.6\,\mathrm{Re}_p^{1/2}\,\mathrm{Pr}^{1/3} \tag{34}$$

where the slip velocity was used to evaluate the Reynolds number.

The mass transfer coefficient was calculated using correlation [28]:

$$\mathrm{Sh}_p \quad 1 \quad \frac{0.752\,\mathrm{Re}_p^{0.472}}{1 \quad (\mathrm{Re}_p\,\mathrm{Sc})^{\ 1}\mathrm{Sc}^{1/3}} \tag{35}$$

The diffusivity of water in air was determined using the correlation [29]:

$$D_g \quad 2.302 \ 10^{\ 5} \ \frac{p}{p_o} \ \frac{T_g \quad 273}{T_o}^{\ 1.81} \tag{36}$$

where $p_o = 0.98 \cdot 10^5$ Pa and $T_o = 256$ K.

The "drying extent" in the draft tube was evaluated from the axial variation of humidity along the draft tube and from the maximum air humidity, y_e:

$$x_A \quad \frac{y \quad y_0}{y_e \quad y_0} \tag{37}$$

where

$$y_e \quad y_0 \quad \frac{G^L_{H_2O0}}{G_{sv}} \tag{38}$$

The heat and mass balance equations were solved over the entire length of the draft tube. The length of the tube was divided into equal increments for the purpose of numerical calculations. It was assumed that the particles were always surrounded by a thin layer of liquid (water, solution or suspension). The axial particle velocity, voidage distribution and axial pressure distribution along the tube were obtained from hydrodynamic model. Input data are: air mass flowrate at the column inlet (G_f), air flowrate through annulus (G_a), particle circulation rate (G_p) and fluid static pressure above the draft tube (p_H). The draft tube entrance conditions are: $y(z = 0) = y_0$, $T_g(z = = 0) = T_{gi} = T_{gci}$ and $T_p(z = 0) = T_{pi} = T_{a0}$ (see Fig. 1).

Proposed model is very similar to the model recently published by Littman *et al.* [30]. The main difference in comparison with Littman *et al*. model lies in hydrodynamic of flowing mixture. Proposed model also neglect interparticle temperature gradient.

Experimental

The drying experiments were conducted in the modified spouted bed unit with draft tube presented in Fig. 3. The drying chamber is cylindrical column D_c = 215 mm i. d. in the lower part and 320 mm i. d. in the upper part. The overall column height is 1500 mm, while the effective column height (above the nozzle) is 1200 mm. Air was introduced into the drying section through the nozzle d_n = 70 mm i. d. (5e, Fig. 3). The base of drying section is conical (45°). The draft tube d_t = 70 mm i. d. and 900 mm in height, was mounted axially above the nozzle with a possibility to change the distance between the top of the nozzle and the draft tube (L, Fig. 1).

The system is equipped with a tank for the slurry with an agitator and with a peristaltic pump as the feeding device. The dried product was separated from the air in a subsequent step by cyclone and bag filter unit. Bag filters cleaning occur in automatic mode in a programmed sequence. Before leaving the system, the air is passed through a packed bed scrubber. The air blower is placed at the end of process line, in such way fluid bed dryer operated under vacuum in order to ambient pressure.

The inert particles were polyethylene beads with an equal volume sphere diameter of 3.3 mm and a particle density of 921 kg/m^3. The estimated inert particle sphericity is 0.9.

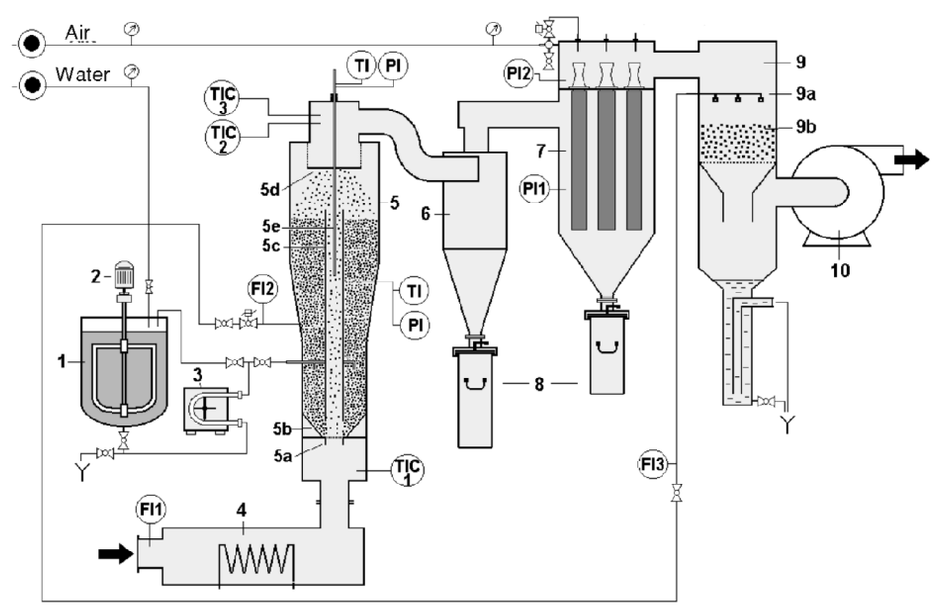

Figure 3. Schematic diagram of the drying system

1 – tank, 2 – agitator, 3 – pump, 4 – air heater, 5 – column, 5a – nozzle, 5b – cone base, 5c – draft tube, 5d – deflector, 5e – movable pressure and temperature probe, 6 – cyclone, 7 – bag filter, 8 – product containers, 9 – scrubber, 9a – water nozzle, 9b – packing, 10 – blower, FI – flowrate indicator, PI – pressure indicator, TIC – temperature indication and control

Overall air flowrate was measured by calibrated orifice connected to a water manometer. The air flowrate in the annulus was measured indirectly, by measuring the pressure gradient in the annulus. To obtain the corresponding velocity there, calibration plot was prepared by measuring the pressure gradient *vs*. velocity relationship in a fixed bed of particles in column 60 mm in diameter. The data are correlated as a relationship between modified friction factor for packed bed and modified particle Reynolds number in the annulus. We assumed that the voidage in the moving bed annulus would be the same as in the fixed bed. The resulting correlation is:

$$f_{pA} \quad 94.7/\,\mathrm{Re}'_{pA} \quad 0.979 \tag{39}$$

The particle circulation rate was determined by measuring tracer particle velocity in the annulus through a glass window and using a relation:

$$G_p \quad \rho_p A_a (1 \quad \varepsilon_a) v_a \tag{40}$$

The drying process in the spouted bed with the draft tube is performed in such a manner that the bed of inert particles is established with hot air, to attain the corresponding temperature regime. The suspension to be dried is introduced into the center of annular zone using four tubes 4 mm in diameter. The suspension is introduced at 400 mm from the bottom (L_f, Fig. 1). Due to intensive circulation of the bed particles, the suspension is dispersed, and a thin film coat of the liquid forms on the surface of the particles. During the residence in the draft tube, the film dries forming a scum of dry material on the particles surface. In the zone above the spout, due to fluid-particle and particle-particle friction, as well as due to the impact with the deflector, positioned above the draft tube, the scum is detached from the particles and carried away in the air stream to the collector. The inert particles fall on the annulus surface and flows downward for the repetitive wetting.

A temperature controller TIC1 maintains the inlet air temperature at the desired level. A thermo controller TIC2, which is situated at the top of the column controls feeding pump (on/off mode) in order to keep the exit air temperature constant. The exit air temperature we call also ”drying” temperature. Thermo controller TIC3, which is also placed at the top of the column, is set at a temperature, which is 20 °C above the drying temperature (TIC2 +20 °C). Its role is to prevent overheating of the bed, in the case of feed pump failure, by introducing pure water into the system.

Temperatures and static pressures in the annulus were recorded at 5 points located at equal distances between $z = 0$ and $z = H$. Temperatures and static pressures in the draft tube were measured by specially designed movable probe placed in the column axis. The suspension flowrate into the column was measured by recording suspension level in slurry tank over certain period of the time. During the experiments, all temperatures were continuously recorded using a PC and data acquisition system.

A total of 15 runs involved two test groups. In the first group, the feed was water while in the second group feed suspensions were calcium carbonate, calcium stearate and Cineb fungicide.

Table 1. Experimental conditions

Run	Feeding material	x_{H_2O}	V_0 m³/h	V_{sus} l/h	T_{gi} °C	T_{gce} °C	G_d/G_f	G_p kg/h	s %
1	Water	–	255.1	4.80	141.1	100.1	0.866	868	–
2		–	251.5	8.35	139.7	82.5	0.861	864	–
3		–	253.6	9.88	134.4	71.6	0.872	936	–
4		–	244.6	6.25	172.3	107.6	0.854	1076	–
5		–	239.8	9.63	176.0	97.3	0.857	1080	–
6		–	239.2	12.68	176.0	79.0	0.863	1044	–
7		–	236.5	12.45	200.0	95.2	0.870	1037	–
8		–	235.9	9.65	200.0	112.6	0.870	986	–
9	Calcium carbonate $CaCO_3$	0.70	256.7	8.84	141.2	101.0	0.912	864	–
10		0.70	247.3	7.41	149.0	86.8	0.860	1109	0.61
11		0.70	244.6	15.55	167.3	103.3	0.871	1224	0.85
12	Calcium stearate	0.82	234.2	19.57	168.3	88.0	0.807	1357	5.04
13		0.82	232.3	10.57	167.5	96.6	0.799	1519	3.47
14	Cineb fungicide $[(CH_2\text{-}NH\text{-}CS_2)_2\text{-}Zn]$	0.75	238.7	23.65	171.0	86.4	0.856	1076	–
15		0.75	220.4	13.96	171.7	107.9	0.848	652	–

Minimum fluidization parameters (U_{mF} and ε_{mF}) required to calculate variational constants for the prediction of the drag coefficients were determined using Ergun equation 31 . Inert particle terminal velocity (U_t) was determined using equations proposed by Kunii and Levenspiel 32 .

Table 1 presents summary of the experimental conditions.

Results and discussion

Figures 4a and 4b shows the calculated values of particle phase velocity, gas phase velocity and slip velocity as a function of the distance from the feeding line for runs 1 and 12. As seen, the highest slip velocity occurs in the lower part of the draft tube. Figure 5 shows the calculated values of voidage for the same runs. Figure 6 gives the comparison between the measured and calculated values of fluid static pressures. The agreement between experimental data and predictions is within 7%. As an example, Table 2 gives the calculated flow parameters at the draft tube beginning and at the draft tube end. Although the overall hydrodynamic conditions for these two runs are similar, particle phase velocity and voidage in Run 12 (feed was calcium stearate) are slightly lower. This is a consequence of significantly higher particle circulation rate in Run 12 (1357 kg/h in Run 12, 868 kg/h in Run 1). Calcium stearate is low viscosity slurry, so that

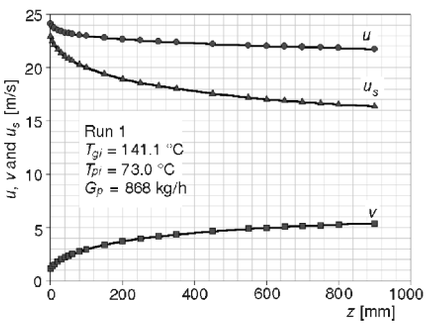

Figure 4a. Axial variation of particle phase velocity, gas phase velocity, and slip velocity in the draft tube, Run 1 (feed: water)

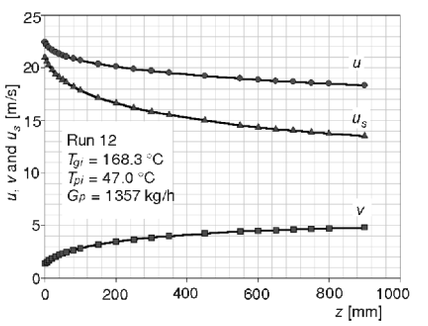

Figure 4b. Axial variation of particle phase velocity, gas phase velocity and slip velocity in the draft tube, Run 12 (feed: calcium stearate slurry)

Table 2. Basic hydrodynamic parameters at the beginning and at the end of the draft tube

	Run 1		Run 12	
	at $z = 0$	at $z = L_t$	at $z = 0$	at $z = L_t$
u m/s	24.12	21.53	21.69	18.22
v m/s	1.18	5.37	1.39	4.81
ε	0.9425	0.9873	0.9234	0.9779
$-dp/dz$ Pa/m	2434	388	3417	472

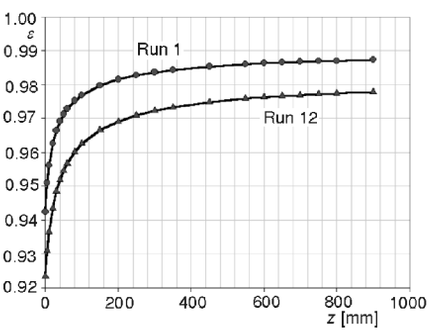

Figure 5. Axial variation of voidage in the draft tube Run 1 (feed: water); Run 12 (feed: calcium stearate slurry)

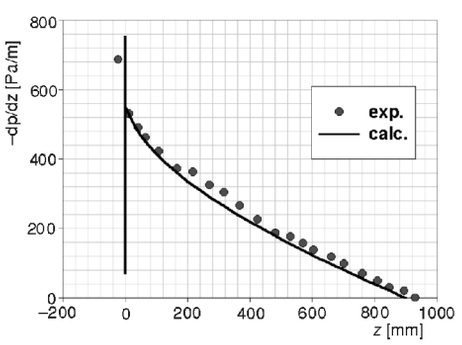

Figure 6a. Draft tube static pressure variation with the distance from the feeding line – comparison between experimental and calculated values, Run 1 (feed: water)

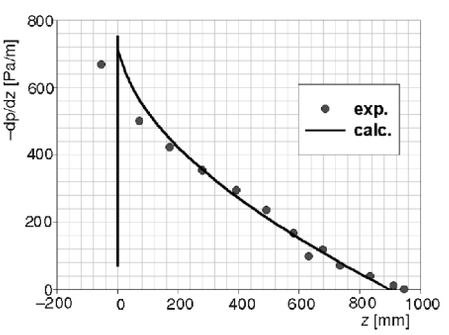

Figure 6b. Draft tube static pressure variation with the distance from the feeding line – comparison between experimental and calculated values, Run 12 (feed: calcium stearate slurry)

overall friction in the dow nward moving packed bed in annulus is much smaller. Figures 7a and 7b shows the calculated values of air temperatures, particle tempe- ratures and wet bulb temperatures as the function of the distance from draft tube inlet. In the same plots, the corresponding experimental values are shown. Evidently, the gas phase gives up its heat more slowly than the particle phase.

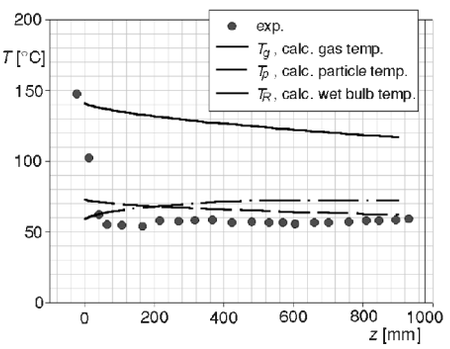

Figure 7a. Temperature distributions in draft tube, Run 1 (feed: water)

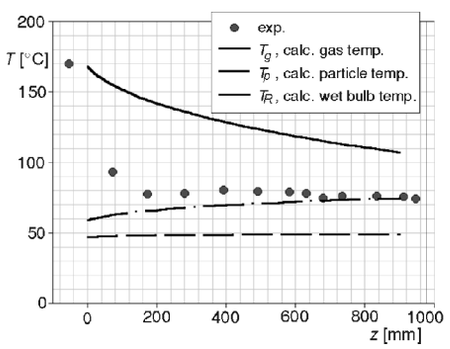

Figure 7b. Temperature distributions in draft tube, Run 12 (feed: calcium stearate slurry)

Figures 8a and 8b shows the amount of water at any height in draft tube. As the water is vaporized, the amount of water in gas phase increases while the amount of water in liquid phase decreases correspondingly. In Run 1 the whole amount of water is vaporized up to $z = 0.550$ m. In Run 10 (feed: calcium carbonate slurry), the calculations shows that whole amount of water is vaporized up to the draft tube end, *i. e*. up to $z = 0.9$ m. Figures 9a and 9b shows the variation of water in draft tube for Runs 2 and 12. In these runs, the feed rate of water (Run 2) or calcium stearate slurry (Run 12) was relatively high so that draft tube length was to short for complete vaporization. The

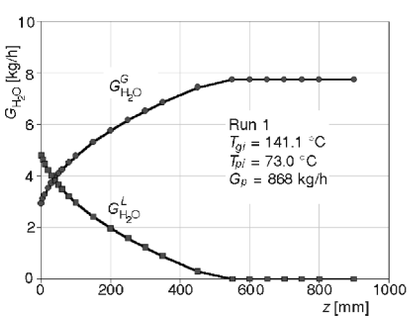

Figure 8a. Water flowrate through draft tube as a function of the distance from the feeding line, Run 1 (feed: water)

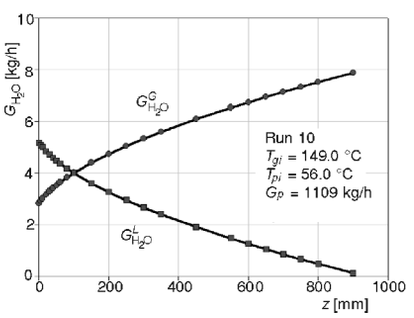

Figure 8b. Water flowrate through draft tube as a function of the distance from the feeding line, Run 10 (feed: calcium carbonate slurry)

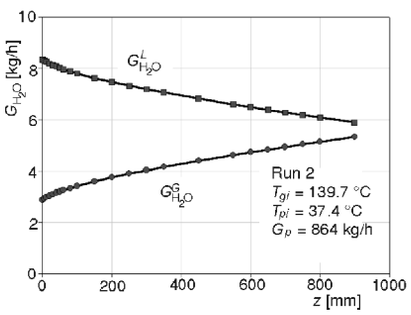

Figure 9a. Water flowrate through draft tube as a function of the distance from the feeding line, Run 2 (feed: water)

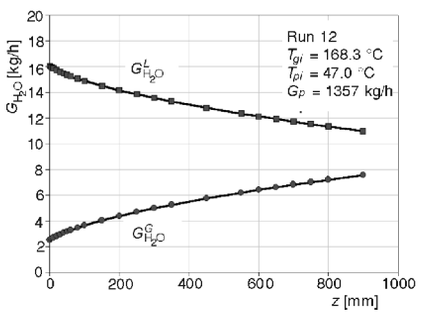

Figure 9b. Water flowrate through draft tube as a function of the distance from the feeding line, Run 12 (feed: calcium stearate slurry)

predictions are in qualitative agreement with visual observations since in these runs water droplets were observed on glass window at the top of the column. The evaporation rate is highest at the beginning of the draft tube, where the driving force is highest and particle velocity smallest. Figure 10 gives the variation of the drying rate with the distance from the feeding line. It is interesting to note that inlet particle temperature has much higher effect on drying rate than inlet gas temperature. This can be seen by comparison of relationships *dy/dz vs. z* for runs 1 and 3 where inlet air temperature is approximately the same. By increasing inlet particle temperature from 32 °C to 73 °C, the initial drying rate increases by a factor 3. On the other side, the increase in inlet air temperature from 134 °C to 200 °C at constant inlet particle temperature has much smaller effect on initial drying rate.

The model can be used to study the effect of operational conditions on overall dryer performance. Figure 11 gives the effect of initial air temperature on the amount of water evaporated in the draft tube, calculated using the data for Run 2. As seen the

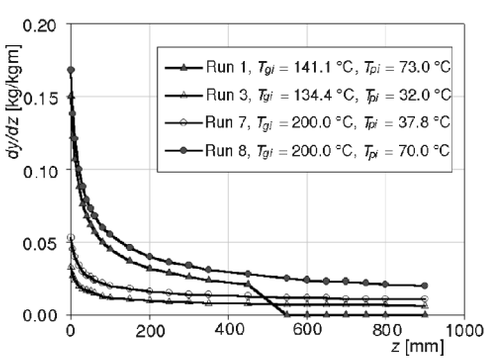

Figure 10. Drying rate as a function of the distance from the feeding line

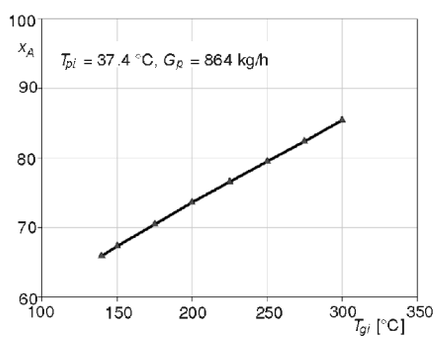

Figure 11. The effect of inlet air temperature on the amount of water evaporated in the draft tube, Run 1 (feed: water)

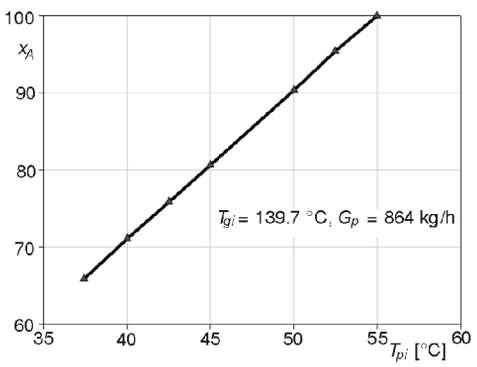

Figure 12. The effect of inlet particle temperature on the amount of water evaporated in the draft tube, Run 2 (feed: water)

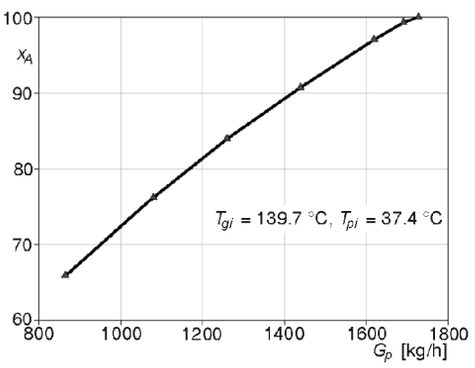

Figure 13. The effect of particle circulation rate on the amount of water evaporated in draft tube, Run 2 (feed: water)

increase in inlet gas temperature for 100 °C increases the amount of water evaporated in the draft tube only by about 13%. On the other side, the increase in inlet particle temperature for 10 °C increases the amount evaporated water by about 20% (Fig. 12). Significant effect has particle circulation rate (Fig. 13). By increase in particle circulation rate by a factor 2, the amount of evaporated water increases from 67% to 100%. Figure 14 gives the draft length required for a complete evaporation of water in the draft tube as a function of inlet air temperature. For the conditions of Run 2 with the draft tube 0.9 m in length the amount of water evaporated in the draft tube is 67%. For complete evaporation the draft tube length should be 2.25 m. By increase in inlet air temperature the required length of the draft tube decreases. Noted examples of calculations illustrate complexity of spouted bed dryer with draft tube. There are many possibilities to obtain desired dryer characteristics. It seems that proposed model can help this job and that can successfully reduce experimental trials.

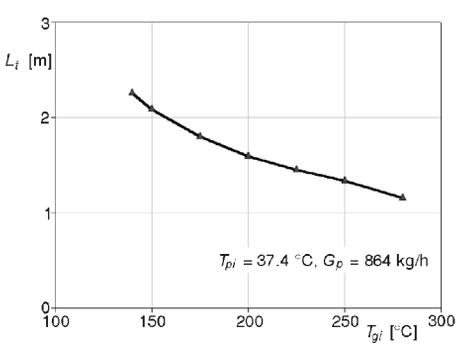

Figure 14. The draft tube length required for complete evaporation in the draft tube as a function of inlet air temperature

We have no possibility to measure air humidity and particle temperature at the end of the draft tube. An indirect test of the quantitative predictions of the model is to measure the air temperature at the column exit assuming that the air flow from the draft tube and from the annulus are well mixed. A comparison between experimen- tal data and the values calculated from the balance:

$$(T_{gce\,calc} \quad G_d(T_{gH})_{mol\,el} \quad \frac{G_a(T_{aH})_{\exp}}{G_f} \tag{41}$$

will give some information's about model accuracy. Figure 15 gives a comparison between experimental values of exit air temperatures and the values calculated from eq. (41). In this calculation T_{aH} is air temperature measured just above annulus top and T_{gH} is calculated value of the air temperature at the end of the draft tube. As seen, most of the calculated values are higher than experimental, 20 °C on average. However, looking only the runs where complete evaporation in draft tube occurs (full symbols), the agreement is better. It is possible that entrained water droplets in other runs affect temperature measurements. It seems that model predictions are reasonable.

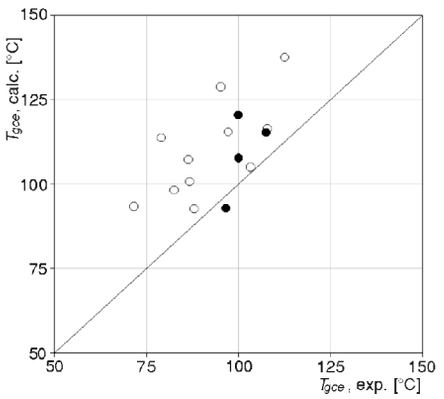

Figure 15. Air temperature at the column exit comparison between experimental and calculated values

Generally, a modified spouted bed dryer with draft tube has a comparable characteristics with fluid bed dryer described in detail in 12 , although motion of inert particle in these two systems is quite different. Required product quality (residual moisture content and active mater content) can be adjusted by selecting appropriate drying temperature. In order to prevent bed sintering in DTSB, the inert particles must be surface dry when they fall back on to the annulus. Important advantage of modified spouted bed dryer is that suspensions and slurries, which contain organic and biological compounds, can be dried. However, this conclusion is not generally valid. Each slurry must be tested at laboratory level. For example, the drying runs with tomato pulp were unsuccessful. It should be noted also that scale-up of DTSB is much more complicated than scale-up of a fluid bed dryer with inert particles.

Limitations of the model

Practical applications of the draft tube spouted and spout-fluidized beds in gas phase system require a relatively short draft tube (typically several meters) and thereby operate hydrodynamically in accelerating flow. Figure 16 gives calculated particle velocity gradient in draft tube as a function of axial distance from the tube inlet. As seen, the drying zone is whole in accelerating region. The plots for all other runs are almost the same. In addition, the calculated acceleration length, defined as a distance

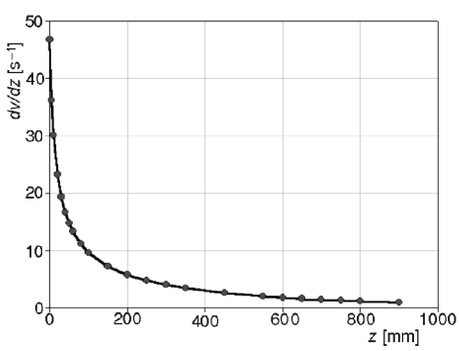

Figure 16. Axial variation of particle velocity gradient in the draft tube, Run 1 (feed: water)

from the tube inlet at which particle velocity reaches 99% of final transport velocity, for all runs is about 1.7 m. This is almost a twice than actual draft tube length in our experimental system (L_t = 0.9 m). Important question is how the constituted relations for the fluid-particle interphase drag coefficient, the fluid-wall friction coefficient and the particle-wall friction coefficient are affected by the acceleration. All of mentioned relationships are derived for steady-state non-accelerating two-phase flow. In addition, the particles in the draft tube are wet. It is reasonable to expect that the presence of liquid phase in draft tube affect friction. Equations (34) and (35) for predicting heat and mass transfer coefficients are essentially derived for a single particle exposed to an non-accelerating flow. Although the voidage in the draft tube is generally high, there are significant differences in the relationship $\varepsilon(z)$ between different runs. In the available literature, there is no data on mass and heat transfer in vertical air-coarse particles flow.

Conclusions

A model for predicting draft tube spouted bed dryer performance is proposed and discussed. Although the model equations are generally applicable for a vertical two-phase dilute flow, the proposed method for predicting the inlet conditions at the feeding line is restricted to the cases where spouted bed type feeding device is used. The spouted bed with the draft tube has complex hydrodynamics. It is apparent that fluid mechanical and mass and heat transfer uncertainties limit model applicability, but predictions seem to be useful for preliminary design and simulation. The major conclusions from our calculations are: (1) The appropriate length and diameter of the draft tube as well as operational conditions for desired performance can be reasonably predicted by the model; (2) The highest evaporation rate occurs in lower portion of the draft tube where slip velocity is also highest; (3) Increasing the inlet air temperature, inlet particle temperature and particle circulation rate increases the rate of evaporation in the draft tube. The effect of increase in inlet air temperature is relatively small indicating the limitations of mass and heat transfer in dilute two-phase flow in draft tube.

A modified spouted bed with draft tube seems to be attractive alternative to a spray dryer. In comparison with fluid bed slurry dryer the main advantage of spouted bed dryer is that drying of some organic and biological materials can be conducted. The most important conditions are that the inert particles must be surface dry when they fall back on to the annulus section to prevent their sticking together and bed sintering.

Nomenclature

a_p – particle surface area per unit volume of the bed (in draft tube), m^2/m^3
A_a – cross-sectional area of the annulus, m^2
A_t – cross-sectional area of the draft tube, m^2
c_{pg} – heat capacity of gas, kJ/kgK
c_{pL} – heat capacity of water, kJ/kg°C

c_{pm} – heat capacity of dried particles, kJ/kgK
c_{ps} – heat capacity of inert particles, kJ/kgK
c_s – particle superficial velocity in draft tube, ($c_s = G_p/\rho_p A_t$), m/s
C_1 – constant in eq. (8)
C_2 – constant in eq. (8)
d_n – diameter of the nozzle, [m]
d_p – inert particle diameter (volumetric), [m]
d_t – diameter of draft tube, [m]
D_c – column diameter, [m]
D_g – diffusivity of water in air, [m^2/s]
f_f – fluid-wall friction coefficient
f_p – particle-wall friction coefficient
f_{pA} – modified friction factor for the flow in the annulus, $\{ f_{pA} = (-dp_a/dz)(d_p/\rho_f U_a^2)\ \varepsilon_a^3/(1-\varepsilon_a)\ \}$
F_D – hydrodynamic drag force per unit volume of suspension, [N/m^3]
F_f – pressure gradient due to the fluid-wall friction, [Pa/m]
F_p – pressure gradient due to the particle-wall friction, [Pa/m]
g – gravitational acceleration, [m/s^2]
G_a – fluid mass flowrate in the annulus, [kg/s]
G_d – fluid mass flowrate in the draft tube, [kg/s]
G_f – fluid mass flowrate at the column inlet, [kg/s]
G_{H_2O} – water mass flowrate in the draft tube, [kg/s]
$G^G_{H_2O}$ – water mass flowrate in draft tube (as gas), [kg/m^{2}s]
$G^L_{H_2O}$ – water mass flowrate in draft tube (as liquid), [kg/m^{2}s]
G_p – particle mass flowrate, [kg/s]
G_{sm} – mass flowrate of dried particles in draft tube, [kg/m^{2}s]
G_{sv} – mass flowrate of dry air in draft tube, [kg/m^{2}s]
h_D – gas-particle mass transfer coefficient, [m/s]
h_p – gas-particle heat transfer coefficient,[W/m^{2}K]
H – packed bed height in the annulus (see Fig. 1), [m]
L – separation length between the bed bottom and draft tube inlet (see Fig. 1), [m]
L_f – vertical coordinate at which the feed is introduced (see Fig. 1), [m]
L_t – length of the draft tube, [m]
M_R – molecular weigth of gas phase, [kg/kgmol]
Nu_p – Nusselt number, ($\mathrm{Nu}_p = h_p d_p/\lambda_g$)
p – static fluid pressure in draft tube, [Pa]
p_a – static fluid pressure in annulus, [Pa]
p_B – partial pressure of water in gas phase, [atm]
p_H – static fluid pressure at the top of the draft tube, [Pa]
p_o – reference pressure in eq. (36), [Pa]
p_S – partial pressure of liquid water, [atm]
Pr – Prandtl number, ($\mathrm{Pr} = \mu c_{pg}/\lambda_g$)
r_{H_2O} – heat of vaporization of water, [kJ/kg]
R – gas constant, [J/kgmol K
Re – Reynolds number in draft tube, based on fluid superficial velocity, ($\mathrm{Re} = d_t \rho_f U/\mu$)
Re_p – particle Reynolds number based on slip velocity, ($\mathrm{Re}_p = d_p \rho_f \mu_s/\mu$)
Re_{pA} – particle Reynolds number for the flow in the annulus, [Re_{pA} $d_p \rho_f U_a$ / (1 ε)]
s – residual moisture content in the product, [%]
Sc – Schmidt number, ($\mathrm{Sc} = \mu/\rho_f D_g$)
Sh_p – particle Sherwood number, ($\mathrm{Sh} = h_D d_p/D_g$)
T_{aH} – gas temperature at the top of the annulus, [°C]
T_{a0} – gas temperature in the centre of the annulus at $z = 0$, [°C]
T_g – gas temperature in draft tube, [°C]

T_{gce} – gas temperature at the column exit, [°C]
T_{gci} – gas temperature in the nozzle (at the column inlet), [°C]
T_{gH} – gas temperature at the end of the draft tube ($z = L_t$), °C
T_{gi} – gas temperature at the entrance of the draft tube ($z = 0$), [°C]
T_o – reference temperature in eq. (36), [K]
T_p – particle temperature in draft tube, [°C]
T_{pH} – particle temperature at the end of the draft tube ($z = L_t$), [°C]
T_{pi} – particle temperature at the entrance of the draft tube ($z = 0$), [°C]
T_R – wet bulb temperature, °C
u – mean interstitial fluid velocity in draft tube ($u = U/\varepsilon$), [m/s]
u_s – slip velocity between fluid and particles, ($u_s = u - v$), [m/s]
U – superficial fluid velocity in draft tube, [m/s]
U_a – superficial fluid velocity in annulus, [m/s]
U_{mF} – superficial fluid velocity at minimum fluidization, [m/s]
U_t – particle terminal velocity in an infinite medium, [m/s]
v – particle velocity in draft draft tube, [m/s]
v_a – particle velocity in the annulus, [m/s]
v_r – radial particle velocity at spout-annulus interface (see Fig. 2), [m/s]
V_{sus} – volumetric flowrate of suspension or slurry, [m³/s]
V_0 – air volumetric flowrate at the column inlet (at 20 °C), [m³/s]
x_A – "drying extent", *i. e.* fraction of water evaporated in the draft tube, eq. (36)
x_{H_2O} – water content in suspension or slurry, (x_{H_2O} kg_{H_2O}/kg_{sus})
y – mass fraction of water in gas phase, (y $kg_{H_2O}/kg_{/dry\ air}$)
y_e – "equilibrium" mass fraction of water in gas phase, eq. (38), (y_e $kg_{H_2O}/kg_{dry\ air}$)
z – vertical coordinate, [m]

Greek letters

β – fluid-particle interphase drag coefficient, [kg/m⁴]
β_{mF} – fluid-particle interphase drag coefficient in a particulately fluidized bed at minimum fluidization, [kg/m⁴]
γ – defined in eq. (17) ($\gamma = \rho_p v^2 - \rho_f u^2$), [kg/ms²]
ε – voidage in the transport tube
ε_a – voidage in the annulus (see Fig. 2)
ε_{mF} – voidage at minimum fluidization
λ – variational constant in eq. (8), Lagrange multiplier
λ_g – thermal conductivity of gas, [W/mK]
μ – viscosity of the fluid,[Ns/m²]
ρ_f – fluid density, [kg/m³]
ρ_p – particle density, [kg/m³]
φ – relative humidity of air
ψ – particle sphericity

Subscripts

0 – refers to feeding line ($z = 0$)

References

[1] Mujumdar, A. S., Drying Technologies of the Future, 10th International Congress of Chemical Enginering, Chemical Equipment Design and Automation – CHISA'90, Praha, Czechoslovakia, 1990, paper P1.3

[2] ***, Handbook of Industrial Drying (A. S. Mujumdar, Ed.), 2nd Edition, Marcel Dekker, New York, 1995.

[3] Kudra, T., Mujumdar, A. S., Advanced Drying Technologies, Marcel Dekker, New York, 2000.

[4] Kudra, T., Mujumdar, A. S., Special Drying Technologies and Novel Dryers, in: Handbook of Industrial Drying (A. S. Mujumdar, Ed.), 2nd Edition, Marcel Dekker, New York, 1995, pp. 1087-1149

[5] Masters, K., Spray Drying Handbook, Halsted Press, New York, 1985.

[6] Povrenović, D. S., Grbavčić, Ž. B., Hadžismajlović, Dž. E., Vuković, D. V., Littman, H., Fluid-Mechanical and Thermal Characteristics of Spout-Fluid Bed Drier with Draft Tube, *Proceedings*, DRYING'91, Elsevier, Amsterdam, 1992, CA 117, pp. 343-351

[7] Hadžismajlović, Dž. E., Povrenović, D. S., Grbavčić, Ž. B., Vuković, D. V., Littman, H., A Spout-Fluid Bed Drier for Dilute Solutions Containing Solids, in: Fluidization VI (J. R. Grace, L. W. Shemilt, M. A. Bergougnou, Eds.), Engineering Foundation, New York, 1989, pp. 277-283

[8] Pham, Q. T., Behaviour of a Conical Spouted-Bed Dryer for Animal Blood, *Can.J.Chem.Eng*., *61* (1983), pp. 426-434

[9] Romankov, P. G., Drying, in: Fluidization (J. F. Davidson, D. Harrison, Eds.), Academic Press, London, 1971, pp. 569-598

[10] Shaw, F. V., Fresh Options In Drying, *Chem.Eng*., July 1994, pp. 76-84

[11] Szentmarjay, T., Pallai, E., Drying of Suspensions In a Modified Spouted Bed Drier with an Inert Packing, *Drying Technol*., *7* (1989), pp. 523-536

[12] Grbavčić, Ž. B., Arsenijević, Z. Lj., Garić-Grulović, R. V., Drying of Suspensions and Pastes In Fluidized Bed of Inert Particles, *J.Serb.Chem.Soc*., *65* (2000), pp. 963-974

[13] Mathur, K. B., Epstein, N., Spouted Beds, Academic Press, New York, 1974.

[14] Epstein, N., Grace, J. R., Spouting of Particulate Solids, in: Handbook of Powder Science and Technology (M. E. Fayed, L. Otten, Eds.), Van Nostrand Reinhold Co., New York, 1984, pp. 507-536

[15] Grbavčić, Ž. B., Vuković, D. V., Jovanović, S. J., Garić, R. V., Hadžismajlović, Dž. E., Littman, H., Morgan, M. H. III, Fluid Flow Pattern and Solids Circulation Rate In a Liquid Phase Spout-Fluid Bed with Draft Tube, *Can.J.Chem.Eng*., *70* (1992), pp. 895-904

[16] Povrenović, D. S., Grbavčic, Z. B., Vuković, D. V., Drying of Suspensions In a Spout-Fluid Bed, *Prehrambeno-tehnol.biotehnol. rev*., *28* (1990), pp. 141-144

[17] Baras, J., Maslić, M., Povrenović, D., Turubatović, L., The Influence of Drying Manner on Indexes of Biological Value of Brewer Yeast, *Proceedings*, 8th European Congress on Biotechnology, Budapest, 1997, p. 73

[18] Povrenović, D. S., Application of Spout-Fluid Bed Drier In Industrial Production, *Proceedings*, DRYING 98, Greece, 1998, Vol. C, pp. 2065-2071.

[19] Grbavčić, Ž. B., Gari}, R. V., Jovanović, S. Dj., Rožić, Lj. S., Hydrodynamic Modeling of Vertical Accelerating Gas-Solids Flow, *Powder Tehnol*., *92* (1997), pp. 155-161

[20] Garić, R. V., Grbavčić, Ž. B., Jovanović, S. Dj., Hydrodynamic Modeling of Vertical Non-Accelerating Gas-Solids Flow, *Powder Tehnol*., *84* (1995), pp. 65-74

[21] Grbavčić, Ž. B., Vuković, D. V., Garić, R. V., Hadžismajlović, Dž. E., Jovanović, S. Dj., Littman, H., Morgan, H., A Variational Model for Prediction Fluid-Particle Interphase Drag Coefficient and Particulate Expansion of Fluidized and Sedimenting Beds, *Powder Technol*., *68* (1991), pp. 199-211

[22] Leung, L. S., in: Fluidization (J. R. Grace, J. M. Matsen, Eds.), Plenum Press, New York, 1980, pp. 25-68

[23] Nakamura, K., Capes, C. E., Vertical Pneymatic Conveying: A Theoretical Study of Uniform and Annular Flow Models, *Can.J.Chem.Eng*., *51* (1973), pp. 39-46

[24] Bird, R. B., Stewart, W. E., Lightfoot, E. N., Transport Phenomena, John Wiley, New York, 1960

[25] Thorley, B., Saunby, J. B., Mathur, K. B., Osberg, B. L., An Analyisis of Air and Solids Flow In a Spouted Beds, *Can.J.Chem.Eng*., *37* (1959), pp. 184-192

[26] Lefroy, G. A., Davidson, J. F., The Mechanics of Spouted Beds, *Trans.Instn.Chem.Eng*., *47* (1969), T120

[27] Ranz, W. E., Friction and Transfer Coefficients for Single Particles and Packed Beds, *J.Chem.Eng.Prog*., *48* (1952), pp. 247-253

[28] Clift, R., Grace, J. R., Weber, M. E., Bubbles, Drop and Particles, Academic Press, London, 1978

[29] Eckert, E. R .G., Drake, R. M., Analysis of Heat and Mass Transfer, McGraw Hill, New York, 1972

[30] Littman, H., Day, J. Y., Morgan, M. H. III, A Model for the Evaporation of Water from Large Glass Particles In Pneumatic Transport, *Can.J.Chem.Eng*., *78* (2000), pp. 124-131
[31] Ergun, S., Fluid Flow Through Packed Columns, *Chem.Eng.Prog*., *48* (1952), pp. 89-94
[32] Kunii, D., Levenspiel, O., Fluidization Engineering, John Wiley, New York, 1969

Authors' addresses:

Z. Arsenijević, R. Garić-Grulović
Institute for Chemistry, Technology and Metallurgy – Centre for Catalysis and Chemical Engineering
Njegoševa 12, 11000 Belgrade, Yugoslavia

Z. B. Grbavčić
Faculty of Technology and Metallurgy, University of Belgrade,
Karnegijeva 4, Belgrade, Yugoslavia

Corresponding author (Z. Arsenijević):
E-mail: zorana@elab.tmf.bg.ac.yu

Paper submited: October 14, 2002
Paper revised: December 14, 2002
Paper accepted: December 27, 200